Otolith phenotypic variability of the blue jack mackerel, *Trachurus picturatus*, from the Canary Islands (NE Atlantic): implications in its population dynamic

Víctor Manuel Tuset[a,*], Alba Jurado-Ruzafa[b], José Luis Otero-Ferrer[c], María Teresa G. Santamaría[b]

[a]*Department of Renewable Resource, Institute of Marine Sciences (CSIC), Passeig Marítim 37-49, Barcelona 08003, Cataluña (Spain)*

[b]*Spanish Oceanographic Institute (IEO),* Canary Oceanographic Centre*, Vía Espaldón, Dársena Pesquera (38180), Santa Cruz de Tenerife (Spain)*

[c]*Universidade de Vigo, Departamento de Ecoloxía e Bioloxía Animal, Campus Universitario de Vigo, Fonte das Abelleiras, s/n 36310, Vigo, Galizia (Spain)*

*Corresponding author at:

E-mail address: vtuset@icm.csic.es (V.M. Tuset)

Department of Renewable Resource, Institute of Marine Sciences (CSIC), Passeig Marítim 37-49, Barcelona 08003, Cataluña (Spain).

Abstract

Studies have described the presence of different population units of blue jack mackerel, *Trachurus picturatus*, in the NE Atlantic region. However, the hypothesis of several populations has been subtly questioned due to the high similarity in the otolith shape among some regions. It suggests the possibility of migrations processes connecting them, especially between Madeira, the Canary Islands and the African coast, being the Canary Islands the region with higher potential of mixing due to the oceanographic conditions. In order to explore this hypothesis, we quantified the phenotypic variability in the otolith contour of the blue jack mackerel from Canary Islands using wavelets as mathematical descriptor. Our findings revealed the presence of three otolith phenotypes (M1, M2 and M3) in similar proportions. They were not linked to sex, age and size, but showed temporal variations associated with spawning, recruitment and feeding seasons. The best model to explain the population structure of *T. picturatus* in the Canary waters was based on local migration triangles and the 'contingent theory', where migrants and residents compose the population. In addition, we estimated different somatic growth parameters linked to these phenotypes. These results suggest a complex population structure in the region with possibility of connectivity with the closest populations inhabiting the Madeira archipelago and the African coast. However, future studies are necessary including the whole Atlantic distribution of the species, with special attention to the seasonal variations in the frequency of these phenotypes to clarify the intraspecific polymorphism and the migratory processes.

Keywords: sagittae, contour analysis, somatic growth, population structure, small pelagic fish

1. Introduction

The stock identification has become a crucial topic for fishery science and management programs (Cadrin *et al*., 2014). A broad spectrum of techniques has been used for this purpose, tending to a holistic approach for increasing the likelihood of success (Begg and Waldman, 1999; Higgins *et al*., 2010; Marengo *et al*., 2017). These techniques have included the estimation of life-history parameters (e.g., growth, mortality, spawning) (Begg *et al*., 1999; Barrios *et al*., 2017), the identification and analysis of natural tags (e.g., body and otolith morphometrics, genetics, parasites, otolith chemical composition) (Thorrold *et al*., 1997; Campana *et al*., 2000; Sturrock *et al*., 2012; Tanner *et al*., 2015), and the use of internal and external markers (i.e., electronic tags, chemical marking) (Nielsen, 1992; Jacobsen and Hansen, 2004; Jepsen *et al*., 2015). The combination of genetic and biological characteristics is currently the most recommended approach (Cadrin *et al*., 2014), although the identification of morphological phenotypes is the most used (Campana and Casselman, 1993; Cardinale *et al*., 2004; Turan, 2006; Stransky *et al.*, 2008; Bacha *et al*., 2014), likely because it is relatively easy, inexpensive and time-efficient tool.

In general, phenotypic analyses are often performed comparing the otolith (Campana and Casselman, 1993; Cardinale *et al*., 2004; Stransky *et al.*, 2008) and body shapes (Turan, 2006; Vasconcelos *et al*., 2017; Pérez-Quiñonez *et al*., 2018). The great advantage of otolith is the continuous incorporation of material and no reabsorption (Gauldie and Nelson, 1990), whereas the plasticity of fish body shape can be reversible through life (Meyer, 1987; Allendorf and Hard, 2009). In both cases, the phenotypic variability reflects an individual/population response to different environmental conditions (e.g., temperature, salinity, food availability, substrate type, depth) (Cardinale *et al.*, 2004; Mérigot *et al*., 2007; Vignon and Morat, 2010) providing insight into events that influence life history of fishes (Campana, 2005; Thorrold *et al*., 2007; Vignon, 2015). Nevertheless, phenotypic variability has a strong genetic component very dependent on the connectivity among populations (Swain and Foote, 1999; Hüssy, 2008; Reichenbacher *et al.*, 2009; Vignon and Morat, 2010; Mahé *et al*., 2016). The most studies have been mainly focused on the quantitative analysis of populations defined at *a priori* spatial scale (local or regional), and the description of the average phenotype (Tuset *et al*., 2003; Javor *et al*., 2011; Ider *et al*., 2017; Vasconcelos *et al*., 2018). This approach assumes that genetic expression of continuous traits (as the morphometry and shape of otolith and fish body) results in phenotypes following a unimodal distribution in each locality (Naish and Hard, 2008). However, a polymorphism may exist induced by fishing pressure (Kuparinen and Merilä, 2007; Allendorf and Hard, 2009; Enberg *et al*., 2009, 2010; Hidalgo *et al*., 2014; Ward *et al*., 2016),

environmental influences (Pigliucci, 2005; Ramler *et al*., 2014; Réveillac *et al*., 2015), simply due to a natural process as feeding efficiency (Skulason *et al*., 1989; Schluter, 1995; Chavarie *et al*., 2016), or different somatic growth rates within population (Rodgveller *et al*., 2017).

The blue jack mackerel, *Trachurus picturatus* (Bowdich, 1825), is a medium pelagic species with high economic value reaching depths beyond 500 m (Denda *et al*., 2017) and inhabiting the central-eastern Atlantic waters, from the Bay of Biscay (France) southward to Mauritania (Jurado-Ruzafa *et al*., 2011, 2019) including Azores, Madeira and the Canary Islands (Macaronesian archipelagos), and eastward into the Mediterranean Sea (Smith-Vaniz and Berry, 1981). Previous studies based on genetic (Zenkin and Ryazantseva, 1987), parasitology (Costa *et al*., 2012, 2013; ICES, 2013, Vasconcelos *et al*., 2017), otolith microchemistry (Moreira *et al*., 2018), and otolith and fish-body shape analysis (Shaboneyev and Ryazantseva, 1977; Vasconcelos *et al*., 2018; Moreira *et al*., 2019a) had concluded that the insular and continental populations were different. However, a recent study has revealed the lack of genetic differentiation between the whole Atlantic and Mediterranean populations (Moreira *et al*., 2019b). In fact, some authors had already suggested the possibility of mixed stocks (Moreira *et al*., 2018, 2019a; Vasconcelos *et al*., 2018). The European Commission is requiring establishing separate quotas in the Macaronesian Atlantic archipelagos (Council Regulation (EU) 2018/120) and, therefore, defining the structure of the entire population in the CE Atlantic is mandatory. In general, *Trachurus* spp. are characterized by a migratory behaviour related to the life cycle (Abaunza, et al., 2003, 2008; Ruas and Vaz-dos-Santos, 2017). To understand their populations structures two population models have been proposed: the 'migration triangle' of Harden Jones (1968) —which illustrates migration circuits throughout the life cycle (Arcos *et al*., 2001; Abaunza *et al*., 2008)—and the metapopulation concept (Levins, 1969, 1970)—with migratory sub-units with different levels of connectivity (Gerlotto *et al*., 2012; Hintzen *et al*., 2014; Bertrand *et al*., 2016; Sassa *et al*., 2016). *A priori* the population structure of *T. picturatus* of the North East Atlantic seems to be enclosed within local migration triangle model (Vasconcelos *et al*., 2018; Moreira *et al*., 2018, 2019a), where continental/islands shelf could function as nursery or growth zone, and offshore (seamount/bank) areas would act as feeding zones (Gomes *et al*., 2001; Arkhipov *et al.*, 2002; Menezes *et al*., 2006).

Small and medium pelagic stocks from the Canary Islands have recently been included in the annual assessment framework of the Fishery Committee for the Eastern Central Atlantic (CECAF) (FAO, 2016). It entails the knowledge on biology and ecology of the species and the correct delimitation of stock boundaries for an adequate status assessment of these populations. Although the population of blue jack mackerel completes its life cycle in Canary archipelago

(Jurado-Ruzafa *et al*., 2011, 2013; Moyano and Hernández-León, 2011), some studies have suggested the possibility of connectivity with other closer populations. In particular, the presence of larvae has been occasionally detected into upwelling filaments from the African coast that reach the Canary Islands (Moyano *et al*., 2009, 2014; Rodríguez *et al*., 2009; Brochier *et al*., 2011), which could represent a complementary source of individuals, making the population structure more complex (John and Zelck, 1997; Moyano and Hernández-León, 2009). Also, some authors have suggested connectivity among the Macaronesian archipelagos, and also with the Portugal mainland due to the high similarity in the chemical composition and shape of otoliths (Vasconcelos *et al*., 2018; Moreira *et al*., 2018, 2019a). However, the possible processes of mixing/connectivity remain unknown. For those reasons, the main goal of the present study was the otolith shape analysis of *T. picturatus* from the Canary Islands (i) to determine the otolith phenotype variability; (ii) to establish if there are seasonal changes in the frequency of these morphotypes, which may indicate migratory process; and (iii) to establish the relationship between phenotypes and somatic growth. The initial hypothesis is that population might be composed of several phenotypes due to nearby with the African coast and Madeira archipelago.

2. Material and methods

2.1. Data sources

The present study was performed using a biological database of blue jack mackerel of the Canary Oceanographic Centre of the Spanish Oceanographic Institute (IEO) in the Canary Islands (Spain). It was composed by 2,472 individuals monthly collected from the commercial landings between March 2005 and March 2006 in the Tenerife Island (NE Atlantic Ocean, Fig. 1), where more than 70% of the annual landings of small pelagic fish in the Canary Islands are performed (EU, 2017). All the specimens were measured for total length (*TL*, 0.1 cm) applying a correction factor for avoiding a size loss by freezing process (Jurado-Ruzafa and Santamaría, 2013). Sex was macroscopically assigned and categorized into three types: juvenile, male and female (Jurado-Ruzafa and Santamaría, 2013). The *sagittae* otoliths were extracted, cleaned, and storage dried in labeled vials for the ageing and morphological studies. However, only otoliths of 472 specimens with the clearest annuli deposition (from 0 to 6 years, see Jurado-Ruzafa and Santamaría, 2018) were considered for our purpose. Finally, the unique data of 6 years-old age was eliminated from subsample to avoid biases.

2.2. Otolith shape analysis

166 The left otoliths were placed with the inner side (*sulcus acusticus*) downward and rostrum
167 to the right (Fig. S1, Supplementary material). They were digitized against a black background
168 using a digital camera coupled to a stereomicroscope at 10× magnification and NIS-Elements
169 F© imaging software. ImageJ 1.50i (http://imagej.nih.gov/ij) was used for taking measurements
170 of otolith length (*OL*, 0.01 mm).
171 The shape was analysed using wavelet functions whose advantage in relation to other
172 contour analyses (i.e., Elliptic Fourier, Fast Fourier Transform or shape indices) is that they
173 enable to identify single morphological points (landmarks) located on the x-axis along the
174 contour, where the *rostrum* is the origin of the contour (Parisi-Baradad *et al*., 2005; Lombarte
175 *et al*., 2006; Sadighzadeh *et al*., 2012). A total of 512 equidistant Cartesian coordinates on each
176 orthogonal projection of the otolith were extracted and analysed using the wavelet transformed
177 (*WLT*; see Parisi-Baradad *et al*., 2005). Image processing was performed using the image
178 analysis software Age and Shape (version 1.0; Infaimon SL©, Barcelona, Spain). Each contour
179 originated nine wavelets depending on the degree of otolith detail (Fig. 2). The 4th wavelet was
180 used in the present study since it is the best scale for the discrimination of stocks (Sadighzadeh
181 *et al*., 2014), related to intraspecific differentiation of otolith phenotypes.
182
183 *2.3. Statistical analysis*
184 A principal component analysis (PCA) based on the variance–covariance matrix was
185 performed to reduce the wavelet functions without losing information (Sadighzadeh *et al*.,
186 2012, 2014; Tuset *et al*., 2015, 2016). To detect the significant eigenvectors, the percentage of
187 total explained variation of eigenvectors *versus* proportion of variance expected under the
188 "broken stick model" was plotted (Frontier, 1976; Gauldie and Crampton, 2002). Intraspecific
189 differences that might be attributed to allometry were tested using Pearson's correlations
190 between otolith length and the principal components (Stransky and MacLellan, 2005; Tuset *et*
191 *al*., 2015). The effect of otolith length was removed using the residuals of the common within-
192 group slopes of the linear regressions of each component on otolith length, building a new PCA
193 matrix (Tuset *et al*., 2015, 2016). The new PCA components were tested for normality and the
194 homogeneity using a permutational multivariate analysis of variance (PERMANOVA;
195 Anderson, 2001) with 9,999 permutations and the Manhattan distance to detect differences
196 sexes.
197 Clustering of otoliths was performed using the *k-means* algorithm with the package *NbClust*
198 in R, a common method for partitioning a dataset into groups of patterns (Hartigan and Wong,
199 1979). It divides data set into a pre-defined *k* number of clusters (here ranging between 2 to 10)

whereby each observation is assigned to the cluster that minimises the distance of that point to the cluster centroid. The most subjective element in *K*-means clustering is the requirement for the input of a predefined number of clusters into the algorithm (Hung *et al*., 2005; Yao *et al*., 2013). To determine the number of clusters (also named 'morphotypes' or 'M') we used the 'all' criteria for obtaining the more common effective solution. To validate the optional solution, several internal and stability measures were obtained for the more probably options using the package *clValid* (Brock *et al*., 2008).

A statistical test of independence (χ^2) was performed to determine the influence of sexes (males and females) on the type of morphotype and to examine possible variations of the frequency of juveniles and adults of each morphotype through the year. For that, the catch date was grouped in three periods following the life cycle proposed for *Trachurus murphyi* (Gerlotto *et al*., 2012) and adapted for *T. picturatus* (Jurado-Ruzafa and Santamaría, 2011, 2013): breeding (January-April), feeding (May-July) and recruitment (August-December). The adult specimens were considered from age-1 since mature specimens were reported from this age (Jurado-Ruzafa and Santamaría, 2013, 2018).

The total length and age of fish were tested for the assumption of normality and homogeneity of variance using the Kolmogorov-Smirnov (*K-S*) test for goodness-of-fit, and Bartlett's test (Zar, 1996), respectively. Since variables were not normally distributed, the comparison of mean values among morphotypes was performed using a non-parametric test (Kruskall Wallis test) (Zar, 1996). To determine whether the fish age and length-frequency distributions differ between them, a Kolmogorov-Smirnov test was used. This test identifies differences between two observed frequency distributions and is particularly sensitive to deviations in skew and kurtosis: hence a Bonferroni correction was employed to account for multiple comparisons among them.

To analyse the disparities in the fish growth parameters among morphotypes, von Bertalanffy growth (VBG) model (Von Bertalanffy, 1938) was fitted:

$$L_t = L_{inf}(1 - e^{-k(t-t0)}) + \varepsilon$$

where L_t is the predicted mean length at age t, L_{inf} is the asymptotic mean length, k is the growth rate, t_0 is the theoretical age at which length is 0, and ε denotes the belief that residuals would be distributed normally about the expected growth line (Haddon, 2001). Starting parameters for the model were determined using a Ford-Walford plot. A Gauss-Newton's algorithm for nonlinear least square procedure was used to estimate the growth parameters. Confidence intervals of growth parameters were calculated via bootstrapping with 1,000 iterations. The fish growth parameters were estimated with the package *FSA* (Ogle, 2016) in R. The comparison of

fish growth parameters among morphotypes was performed without fixed variables, fixing one, two or the three parameters and using Akaike's Information Criterion (AIC) to investigate the robustness models. In particular, the ΔAIC value was used (ΔAIC= 0) to find the 'best' model, which is the difference between the AIC value for each model and the lowest observed ΔAIC value. Moreover, models with AIC values differing by less than 2 were considered equally plausible (Burnham and Anderson, 2002).

All statistical analyses and graphical representations were conducted with the software R (R Core Team, 2016).

3. Results

3.1. Otolith phenotypic variability

The first 27 principal components of the PCA analysis accounted for higher variance than expected by chance alone (93.1%), but only the first six components reached values above 5% of the variance (Table S1, Supplementary material). The PERMANOVA analysis did not indicated significant differences in the otolith shape between sexes ($F_{1, 470}$=1.242, p= 0.217).

The result of *K*-means analysis suggested the presence of 2 or 3 morphotypes as the best option interpreting the distribution data (Fig. S1, Supplementary material). However, the validation measures clearly showed that the best solution was the selection of 3 morphotypes (M1, M2 and M3) (Table S1, Supplementary material). Assuming this premise, the positive values of PC1 axis (20.4% of variance explained) represented a lanceolated shape (M2) *versus* a more elliptic pattern (M3) characterized by a wider and more concavity of dorsal-ventral margin (Figs. 3a, b) (Fig. S3, Supplementary material). The density distributions of the three morphotypes showed a skewed unimodal pattern linked to the standard phenotype described before. The negative records of PC2 axis (12.6% of variance) differentiated the otoliths with a peaked *antirostrum* (M2 and M3); whereas the positive values identified otolith with an *antirostrum* absent or few developed (M1) (Figs. 3a, b) (Fig. S3, Supplementary material). For this space, the density distribution of M3 exhibited a skewed unimodal pattern, whereas the M1 and M2 displayed skewed bimodal patterns. These results indicated that the *antirostrum* size was different among the three phenotypes. In addition, the PC5 and PC6 axis discerned the posterior margin of otolith in angled or oblique (Fig. S3, Supplementary material).

3.2. Seasonal variability of phenotypes

There was no difference in the frequency of males and females among phenotypes (χ^2= 3.189, df=2, p=0.203). However, the adult/juvenile proportions in each morphotype were not

independent of the life cycle (χ^2= 37.421, χ^2= 69.428, χ^2= 31.433; *df*= 2 and $p< 0.001$ for M1, M2 and M3, respectively). Juveniles were mainly detected in the recruitment period, although they also predominated during the feeding period for the M1 and breeding season for M2 and M3 (Fig. 4). A high relative frequency of adult fish for the three morphotypes was observed during the feeding period (>55%), which noticeably decreased in the spawning time (Fig. 4).

3.3. Linking phenotypes with fish growth

Although there were no significant differences in the age and total length average among morphotypes (Table 1), significant variations were detected in the distribution of M1 *versus* M2 (K-S test, Z= 0.166, p= 0.020 for age; Z= 0.202, p= 0.001 for total length) and M3 (K-S test, Z= 0.194, p= 0.007 for age; Z= 0.239, $p< 0.001$ for total length) (Fig. 5). In contrast, the structure was similar for M2 and M3 (K-S test, Z= 0.208, p= 0.003 for age; Z= 0.068, p= 0.877 for total length) (Fig. 5).

Three models of fish growth were selected on the basis of ΔAIC value (Table S3). The best model (ΔAIC= 0) indicated a differential growth linked to the morphotypes described (Table 2). In this case, the VBG parameters with the lowest growth rate (k=0.143 years^{-1}) and highest asymptotic length (L_{inf} = 40.95 cm *TL*) were estimated for specimens with M2; whereas the fastest growth (k=0.321years^{-1}) and lowest asymptotic length (L_{inf} = 29.94 cm *TL*) were attained for individuals with M3. However, models fixing L_{inf} (ΔAIC= 0.5) or k (ΔAIC= 1.6) were also plausible, attaining smaller growth parameters the morphotypes M2 and M3 (Table 2).

4. Discussion

The present study demonstrated that *T. picturatus* from the Canary Islands present variability in the otolith shape. The analytical methods revealed the presence three phenotypes (M1, M2 and M3), which were independent of sex and age. Their identification was based on well-defined features: the presence/absence of *antirostrum* and notch in the *excisura ostii*, and the type of curvature of the dorsal-posterior and ventral margins. However, the skewed (asymmetrical) distribution of morphotypes (see PC1 axis, Fig. 3) and the bi-modal distribution noted in the M1 and M2 (see PC2 axis, Fig. 3) might question the suitability of the results obtained. In this sense, the tails of distribution were related to contour irregularities, whereas the bi-modal pattern illustrated the morphological variability in the *antirostrum* zone (e.g., more pointed *versus* blunt, or the degree of convexity of margin when *antirostrum* is absent/present). This representation of specific details is a particular quality of wavelets (Parisi-Baradad *et al*.,

2005) *versus* Elliptic Fourier (Moreira *et al*., 2019a), but these features are certainly inconsistent for the partitioning of patterns.

Although the phenotypic variability described in the present study has been already shown in other studies (Vasconcelos *et al*., 2006; Moreira *et al*., 2019a) and websites (AFORO; www.isis.cmima.csic.es/aforo/; Lombarte *et al.,* 2006), its frequency is unexplored for all the Atlantic and Mediterranean populations. For that reason, our findings open a new perspective on the population structure of *T. picturatus* and reinforce the idea that any fishing management scenario should require a more exhaustive phenotypic knowledge for a more precise understanding of the population dynamics. Besides, they may be useful to anticipate how populations respond to natural and anthropogenic processes (Ward *et al*., 2016).

4.1. Population structure

The seasonal variation of juveniles and adults through annual cycle suggested a population model based on local migration triangles (Gomes *et al*., 2001; Arkhipov *et al.*, 2002; Menezes *et al*., 2006). The low relative abundance of adults during the recruitment period would be due to a migratory behaviour towards deeper-waters for feeding. After, they would move into coastal waters for spawning and would remain feeding inshore before returning to seamounts. Juveniles would inhabit in coastal areas and be more abundant in the recruitment and breeding seasons since the peak spawning is around February (Jurado-Ruzafa and Santamaría, 2011, 2013). However, juveniles with phenotype M1 showed an alternative pattern declining during the breeding season and noticeably increasing during the feeding period. One possible explanation of those specific differences may be the existence of behavioural groups with distinct circuits that mix during certain seasons and life history stages. Considering this hypothesis, the population structure of *T. picturatus* from the Canary Islands may be closer to the 'contingent theory' (Secor 1999, 2002, 2005), according to which, coexisting migratory and resident contingents (understood as a group of individuals) with different capabilities and life-cycle patterns (ICES, 2007) would coexist. In fact, secondary spawning and recruitment areas in oceanic waters are considered in *T. murphyi* (Gerlotto *et al*., 2012), and aggregations of spawners have been observed offshore of the Azores in *T. picturatus* (Arkhipov *et al*., 2002), as occur in other fish species (Keating *et al*., 2014). The 'contingent theory' considers that a simple migration triangle only represents one contingent in a sympatric complex of contingents. Thus, the population contains several different sets of individuals with natal homing behaviours directed toward different natal locations. In this scenario, phenotypes M2 and M3 may correspond to a contingent developing its life cycle closer inshore (Jurado-Ruzafa and

Santamaría, 2011, 2013; Moyano and Hernández-León, 2011), whereas the phenotype M1 may represent a contingent with a more offshore life style with phases closer to the coast.

4.2. Implications of phenotypic variability

The intraspecific variations in otolith shape (e.g., convexity) response to specific exogenous factors (Hüssy, 2008; Tuset *et al*., 2015), whereas the *rostrum* and *antirostrum* size are linked to genetic variations (Reichenbarcher *et al*., 2009; Vignon and Morat, 2010; Radharkrishnan *et al*., 2012; Reichenbarcher and Reichard, 2014). Nevertheless, the presence of similar phenotypes in populations across the NE Atlantic and the Mediterranean (Lombarte *et al*., 2006; Vasconcelos *et al*., 2006; Moreira *et al*., 2019a) is not consistent with a partial genetic isolation, which was recently rejected by Moreira *et al*. (2019b). Thus, the possibility of variations in the somatic growth related to differential behaviour may be an option more plausible as occurs in other fish species (Karlou-Riga, 2000; Tuset *et al*., 2016; Rodgveller *et al*., 2017). Moreover, the presence of *antirostrum* has been related to shallower coastal habitat and the formation of large fish aggregations with local movements (Vignon, 2012).

Theoretically, the slower growing individuals have larger (elongated) otoliths than faster growing fishes of the same size (Secor and Dean, 1989; Reznick *et al*., 1989; Francis *et al*., 1993; Worthington *et al*., 1995; Tuset *et al*., 2004). From the three plausible models of fish growth obtained, only the non-fixing model perfectly correlated the fish and otolith growth: slower growing individuals (M2) would have elongated otoliths and faster growing individuals (M3) would present elliptic otoliths. Certainly, the fish and otolith growth depends on the prey availability and type. The slower growing individuals swim more efficiently increasing food availability leading to larger size and fitness avoiding adverse environmental conditions, whereas faster-growth fishes intake more prey reaching more quickly age/size at maturation and achieving higher recruitments (Chapman *et al*., 2012a,b; Gillanders *et al*., 2015). Specimens of *T. picturatus* with smaller mouth ingest mainly copepods and amphipods, whereas individuals with larger mouth capture more highly mobile prey as fish (Cuscó, 2015). However, the main problem of non-fixing model was the high value of L_{inf} for M2 (40.95 cm TL) since the largest fish was 28.9 cm TL, which also occurred in the Azores population (García *et al*., 2014). Jurado-Ruzafa and Santamaría (2018) argued that larger specimens might be found in areas that are not exploited by the artisanal purse-seine fleet, which undertakes daily trips close to the coast around the Canary archipelago. We think that these morphotypes reflect variations in the fish growth rates, but the estimated von Bertalanffy growth parameters in the

present study should not be used for other purposes such as fishing assessment due to low number of specimens by case.

5. Conclusions

The phenotypic variability on the otolith shape of *T. picturatus* from the Canary Islands reveals a population composed by specimens, likely with different life history traits. The most plausible explanation to outline population structure is a spatial model based on the 'contingent theory'; however, this model would require further analysis for its confirmation (i.e., telemetric techniques). Assuming this theory, the mechanisms underlying the migratory process should be understood both within the specific context of each island as in the whole Canary archipelago. In any case, we do not dismiss a regional connectivity by larvae transport or oceanic migration, as several authors have suggested (Vasconcelos *et al*., 2018; Moreira *et al.*, 2019a). In fact, Vasconcelos *et al*. (2018) emphasized that an accurate assessment of *T. picturatus* in overall Atlantic area would be necessary to implement the knowledge on migratory processes (vertical and/or horizontal) for detecting the location and time of year when mixing of stocks occurs. Moreover, the comparative studies among regions should be careful in the sampling scheme and in the otolith age-interpretation. Therefore, the discrepancies found at a regional scale should be taken with caution. Finally, the possible presence of mixed populations in the artisanal small pelagic fishery in the Canary Islands constitutes a huge challenge to design an appropriate managing strategy, even more in the current climate change scenario. Besides, this kind of scientific studies should be performed for other exploited small pelagic fish inhabiting waters around the Canary Islands, due to it is more than probable that similar situations are occurring for other species. The results here presented open a wide range of opportunities for further studies which will need the coordinated work to clarify the dynamics of this species, not only at a local, but also at the regional scale.

Acknowledgements

Authors would like to thank all the colleagues from the Canary Oceanographic Center (IEO) who participated in the samples collection and fish biological samplings. The authors wish also to thank two anonymous referees for their helpful suggestions.

References

403 Abaunza, P., Gordo, L., Karlou-Riga, C., Murta, A., Eltink, A.T.G.W., García Santamaría, M.T., Zimmermann,
404 C., Hammer, C., Lucio, P., Iversen, S.A., Molloy, J., Gallo, E., 2003. Growth and reproduction of horse
405 mackerel, *Trachurus trachurus* (Carangidae). Rev. Fish Biol. Fish. 13 (1), 27–61.
406 Abaunza, P., Murta, A.G., Campbell, N., Cimmaruta, R., Comesaña, A.S., Dahle, G., García Santamaría, M.T.,
407 Gordo, L.S., Iversen, S.A., MacKenzie, K., Magoulas, A., Mattiucci, S., Molloy, J., Nascetti, G., Pinto, A.L.,
408 Quinta, R., Ramos, P., Sanjuan, A., Santos, A.T., Stransky, C., Zimmermann, C., 2008. Stock identity of
409 horse mackerel (*Trachurus trachurus*) in the northeast Atlantic and Mediterranean Sea: integrating the results
410 from different stock identification approaches. Fish. Res. 89, 196–209.
411 Allendorf, F.W., Hard, J.J., 2009. Human-induced evolution caused by unnatural selection through harvest of wild
412 animals. Proc. Natl Acad. Sci. USA. 106, 9987–9994.
413 Anderson, M.J., 2001. A new method for non-parametric multivariate analysis of variance. Austral Ecol. 26, 32–
414 46.
415 Arcos, D.A., Cubillos, L.A., Núñez, S.P., 2001. The jack mackerel fishery and El Niño effects off Chile. Progr.
416 Oceanogr. 49, 597–617.
417 Arkhipov, A.G., D.A. Kozlov, V.N. Shnar, Sirota, A.A., 2002. Structure of waters and distribution of fish at
418 different ontogenetic stages around seamounts of Central-Eastern Atlantic Ocean. ICES CM 2002/M:03, 1–
419 15.
420 Bacha, M., Jemaa, S., Hamitouche, A., Rabhi, K., Amara, R., 2014. Population structure of the European anchovy,
421 *Engraulis encrasicolus*, in the SW Mediterranean Sea, and the Atlantic Ocean: evidence from otolith shape
422 analysis. ICES J. Mar. Sci. 71, 2429–2435.
423 Barrios, A., Ernande, B., Mahé, K., Trenkel, V., Rochet, M.J., 2017. Utility of mixed effects models to inform the
424 stock structure of whiting in the northeast Atlantic Ocean. Fish. Res. 190, 132–139.
425 Begg, G.A., Waldman, J.R., 1999. An holistic approach to fish stock identification. Fish. Res. 43**,** 35–44.
426 Begg, G.A., Hare, J.A., Sheehan, D.D., 1999. The role of life history parameters as indicators of stock structure.
427 Fish. Res. 43, 141–163.
428 Bertrand, A., Habasque, J., Hattab, T., Hintzen, N.T., Oliveros-Ramos, R., Gutiérrez, M., Demarcq, H., Gerlotto,
429 F., 2016. 3-D habitat suitability of jack mackerel *Trachurus murphyi* in the Southeastern Pacific, a
430 comprehensive study. Prog. Oceanogr. 146, 199–211.
431 Brochier, T., Mason, E., Moyano, M., Berraho, A., Colas, F., Sangrà, P., Hernández-León, S., Ettahiri, O., Lett,
432 C., 2011. Ichthyoplankton transport from the African coast to the Canary Islands. J. Mar. Syst. 87, 109–122.
433 Brock, G., Pihur, V., Datta, S., Datta, S., 2008. clValid, an R package for cluster validation. J. Stat. Softw. 25, 1–
434 22.
435 Burnham, K., Anderson, D., 2002. Model selection and multimodel inference: a practical information-theoretic
436 approach. Springer-Verlag, New York.
437 Cadrin, S.X., Kerr, L.A., Mariani, S., 2014. Interdisciplinary evaluation of spatial population structure for
438 definition of fishery management units, in: Cadrin, S.X., Kerr, L.A., Mariani, S. (Eds.), Stock Identification
439 Methods: Applications in Fisheries Science, 2nd edition. Elsevier, London, pp. 535–552.
440 Campana, S.E., 2005. Otolith elemental composition as a natural marker of fish stocks, in: Cadrin, S.X., Friedland,
441 K.D., Waldman, J.R. (Eds.), Stock identification methods. Academic Press, New York, pp. 227–245.
442 Campana, S.E., Casselman, J.M., 1993. Stock discrimination using otolith shape analysis. Can. J. Fish. Aquat. Sci.
443 50, 1062–1083.
444 Campana, S.E., Chouinard, G.A., Hanson, J.M., Frechet, A., Brattey, J., 2000. Otolith elemental fingerprints as
445 biological tracers of fish stocks. Fish. Res. 46, 343–357.
446 Cardinale, M., Doering-Arjes, P., Kastowsky, M., Mosegaard, H., 2004. Effects of sex, stock and environment on
447 the shape of known-age Atlantic cod (*Gadus morhua*) otoliths. Can. J. Fish. Aquat. Sci. 61, 158–167.
448 Chavarie, L., Howland, K., Venturelli, P., Kissinger, B.C., Tallman, R., Tonn, W., 2016. Life-history variation
449 among four shallow-water morphotypes of lake trout from Great Bear Lake, Canada. J. Great Lakes Res. 42,
450 421-432.
451 Chapman, B.B., Hulthén, K., Brodersen, J., Nilsson, P.A., Skov, C., Hansson, L.A., Brönmark, C., 2012a. Partial
452 migration in fishes: causes and consequences. J. Fish Biol. 81, 456–478.
453 Chapman, B.B., Skov, C., Hulthén, K., Brodersen, J., Nilsson, P.A., Hansson, L.A., Brönmark, C., 2012b. Partial
454 migration in fishes: definitions, methodologies and taxonomic distribution. J. Fish Biol. 81, 479–499.
455 Costa, G., Melo-Moreira, E., Pinheiro de Carvalho, M.A.A., 2012. Helminth parasites of the oceanic horse
456 mackerel *Trachurus picturatus* Bowdich 1825 (Pisces: Carangidae) from Madeira Island, Atlantic Ocean,
457 Portugal. J. Helminthol. 86, 368–372.
458 Costa, G., Santamaria, M.T.G., Vasconcelos, J., Perera, C.B., Melo-Moreira, E., 2013. Endoparasites of *Trachurus*
459 *picturatus* (Pisces: Carangidae) from the Madeira and Canary Islands: selecting parasites for use as tags. Sci.
460 Mar. 77 (1), 61–68.
461 Cuscó, R. 2015. Aportación al conocimiento de la biología del chicharro (*Trachurus picturatus*, Bowdich (1825);
462 Pisces, Carangidae) en aguas de las Islas Canarias. Thesis Doctoral, Las Palmas de Gran Canaria.
463 Denda, A., Stefanowitsch, B., Christiansen, B., 2017. From the epipelagic zone to the abyss: Trophic structure at

464 two seamounts in the subtropical and tropical Eastern Atlantic - Part II Benthopelagic fishes. Deep-Sea Res.
465 I 130, 78–92.
466 Enberg, K., Jørgensen, C., Dunlop, E.S., Heino, M., Dieckmann, U., 2009. Implications of fisheries-induced
467 evolution for stock rebuilding and recovery. Evol. Appl. 2, 394–414.
468 Enberg, K., Jørgensen, C., Mangel, M., 2010. Fishing-induced evolution and changing reproductive ecology of
469 fish: the evolution of steepness. Can. J. Fish. Aquat. Sci. 67, 1708–1719.
470 EU, 2017. Report of the Regional Co-ordination Meeting for the Long Distance Fisheries (RCM LDF), 2017.
471 Hamburg, Germany, Thünen Institute.
472 EU, 2018/120. Council regulation fixing for 2018 the fishing opportunities for certain fish stocks and groups of
473 fish stocks, applicable in Union waters and, for Union fishing vessels, in certain non-Union waters, and
474 amending Regulation (EU) 2017/127.
475 FAO, 2016. Fishery Committee for the Eastern Central Atlantic, report of the seventh session of the scientific sub-
476 committee, 14–16 October 2015, Tenerife. *FAO Fisheries and Aquaculture Reports* 1128. Rome: FAO.
477 Francis, M.P., Williams, N.W., Price, A.C., Pollard, S., Scott, S.G., 1993. Uncoupling of otolith and somatic
478 growth in *Pagrus auratus* (Sparidae). Fish. Bull. 91, 159–164.
479 Frontier, S., 1976. Étude de la decroissance des valeurs propers dans une analyze en composantes principales:
480 comparison avec le modèle de baton brisé. J. Exp. Mar. Biol. Ecol. 25, 67–75.
481 García, Al., Pereira, J.G., Canha, Â., Reis, D., Diogo, H., 2015. Life history parameters of blue jack mackerel
482 *Trachurus picturatus* (Teleostei: Carangidae) from north-east Atlantic. J. Mar. Bio. Ass. UK. 95(2), 401–410.
483 Gauldie, R.W., Nelson, D.G.A., 1990. Otolith growth in fishes. Comp. Biochem. Physiol. A 97, 119–135.
484 Gauldie, R.W., Crampton, J.S., 2002. An eco-morphological explanation of individual variability in the shape of
485 the fish otolith: comparison of the otolith of *Hoplostethus atlanticus* with other species by depth. J. Fish. Biol.
486 60, 1204–1221.
487 Gerlotto, F., Gutiérrez, M., Bertrand, A., 2012. Insight on population structure of the Chilean jack mackerel
488 (*Trachurus murphyi*). Aquat. Living Resour. 25, 341–355.
489 Gillanders, B.M., Izzo, C., Doubleday, Z.A., Ye, Q., 2015, Partial migration: growth varies between resident and
490 migratory fish. Biol. Lett. 11, 20140850.
491 Gomes, M.C., Serrão, E., Borges, M., 2001. Spatial patterns of groundfish assemblages on the continental shelf of
492 Portugal. ICES J. Mar. Sci. 58 (3), 633–647.
493 Haddon, M., 2001. Modeling and Quantitative Methods in Fisheries. Chapman and Hall, Crc. Boca Raton.
494 Harden-Jones, F., 1968. Fish Migration. Edward Arnold Ltd, London.
495 Hartigan, J.A., Wong, M.A., 1979. A K-means clustering algorithm. Appl. Stat. 28, 100-108.
496 Hidalgo, M., Olsen, E.M., Ohlberger, J., Saborido-Rey, F., Murua, H., Piñeiro, C., Stenseth, N.C., 2014.
497 Contrasting evolutionary demography induced by fishing: the role of adaptive phenotypic plasticity. Ecol.
498 Appl. 24, 1101–1114.
499 Higgins, R.M., Danilowicz, B.S., Balbuena, J.A., Danielsdottir, A.K., Geffen, A.J., Meijer, W.G., Modin, J.,
500 Montero, F.E., Pampoulie, C., Perdiguero-Alonso, D., Schreiber, A., Stefansson, M.O., Wilson, B., 2010.
501 Multi-disciplinary fingerprints reveal the harvest location of cod *Gadus morhua* in the northeast Atlantic.
502 Mar. Ecol. Prog. Ser. 40, 197–206.
503 Hintzen, N.T., Corten, A., Gerlotto, F., Habasque, J., Bertrand, A., Lehodey, P., Brunel, T., Dragon, A.C., Senina,
504 I., 2014. Hydrography and jack mackerel stock in the South Pacific. Final report. IJmuiden, IMARES
505 C176/14, 65pp.
506 Hung, M.C., Wu, J., Chang, J.H., Yang, D.L., 2005. An Efficient k-Means Clustering Algorithm Using Simple
507 Partitioning. J. Inf. Sci. Eng. 21 (6), 1157–1177.
508 Hüssy, K., 2008. Otolith shape in juvenile cod (*Gadus morhua*): ontogenetic and environmental effects. J. Exp.
509 Mar. Biol. Ecol. 364, 35–41.
510 Ider, D., Ramdane, Z., Mahé, K., Duffour, J.L., Bacha, M., Amara, R., 2017. Use of otolith-shape analysis for
511 stock discrimination of *Boops boops* along the Algerian coast (southwestern Mediterranean Sea). Afr. J. Mar.
512 Sci. 39 (3), 251–258.
513 ICES, 2007. Report of the Workshop on Testing the Entrainment Hypothesis (WKTEST), 4–7 June 2007, Nantes,
514 France. ICES CM 2007/LRC: 10 pp.
515 ICES, 2013. World Conference on Stock Assessment Methods (WCSAM), 15–19 July 2013, Boston, USA. ICES
516 CM 2013/ACOM/SCICOM:02. 59 pp.
517 Jacobsen, J.A., Hansen, L.P., 2004. Conventional tagging methods in stock identification: internal and external
518 tags. ICES ASC 2004/EE, 1–29.
519 Javor, B., Lo, N., Vetter, R. 2011. Otolith morphometrics and population structure of Pacific sardine (*Sardinops*
520 *sagax*) along the west coast of North America. Fish. Bull. 109, 402–415.
521 John, H.C., Zelck, C., 1997. Features, boundaries and connecting mechanisms of the Mauritanian Province
522 exemplified by oceanic fish larvae. Helg. Meer. 51, 213–240.
523 Jurado-Ruzafa, A., Santamaría, M.T.G., 2011. Notes on the recruitment of the blue jack mackerel *Trachurus*

524 *picturatus* (Bowdich, 1825) off the Canary Islands (Carangidae, Perciformes). Vieraea 39, 219–224.
525 Jurado-Ruzafa, A., Santamaría, M.T.G., 2013. Reproductive biology of the blue jack mackerel, *Trachurus*
526 *picturatus* (Bowdich, 1825), off the Canary Islands. J. Appl. Ichthyol. 29, 526–531.
527 Jurado-Ruzafa, A., Santamaría, M.T.G., 2018. Age, growth and natural mortality of blue jack mackerel *Trachurus*
528 *picturatus* (Carangidae) from the Canary Islands, Spain (NW Africa). Afr. J. Mar. Sci. 40(4), 451–460.
529 Jurado-Ruzafa, A., Carrasco, M.N., Duque, V., Sancho, A., Hernández, E., Pascual, P.J., Santamaría, M.T.G.,
530 2011. Preliminary data on horse mackerel (*Trachurus* spp.) landings from Mauritanian waters. Mediterranea.
531 Serie de estudios Biológicos II (Núm. especial), 1–30.
532 Jurado-Ruzafa, A., González-Lorenzo, G., Jiménez, S., Sotillo, B., Acosta, C., Santamaría, M.T.G., 2019. Seasonal
533 evolution of small pelagic fish landings index in relation to oceanographic variables in the Canary Islands
534 (Spain). Deep-Sea Res. II. 159, 84–91.
535 Jepsen, N., Thorstad, E.B., Havn, T., Lucas, M.C., 2015. The use of external electronic tags on fish: an evaluation
536 of tag retention and tagging effects. Anim. Biotelem. 3, 1–23.
537 Karlou-Riga, C., 2000. Otolith morphology and age and growth of *Trachurus mediterraneus* (Steindachner) in the
538 Eastern Mediterranean. Fish. Res. 46, 69–82.
539 Keating, J.P., Brophy, D., Officer, R.A., Mullins, E., 2014. Otolith shape analysis of blue whiting suggests a
540 complex stock structure at their spawning grounds in the northeast Atlantic. Fish. Res. 157,
541 Kuparinen, A., Merilä, J., 2007. Detecting and managing fisheries-induced evolution. Trends Ecol. Evol. 22, 652–
542 659.
543 Levins, R., 1969. Some demographic and genetic consequences of environmental heterogeneity for biological
544 control. Bull. Entomol. Soc. Am. 15, 237–240.
545 Levins, R., 1970. Extinction, in: Gertenhaber, M. (Ed.), Some mathematical problems in biology. American
546 Mathemartical Society, Providence, RI, pp. 75-107.
547 Lombarte, A., Chic, Ò., Parisi-Baradad, V., Olivella, R., Piera, J., García–Ladona, E., 2006. A web-based
548 environment from shape analysis of fish otoliths. The AFORO database. Sci. Mar. 70, 147–152.
549 Marengo, M., Baudouin, M., Viret, A., Laporte, M., Berrebi, P., Vignon, M., Marchand, B., Durieux, E.D.H.,
550 2017. Combining microsatellite, otolith shape and parasites community analyses as a holistic approach to
551 assess population structure of *Dentex dentex*. J. Sea Res. 128 (Supplement C), 1–14.
552 Mahé, K., Oudard, C., Mille, T., Keating, J., Gonçalves, P., Clausen, L.W., Petursdottir, G., Rasmussen, H.,
553 Meland, E., Mullins, E., Schon, P.J., McCorriston, P., Pinnegar, J. K., Hoines, Å., Trenkel, V.M., 2016.
554 Identifying blue whiting (*Micromesistius poutassou*) stock structure in the Northeast Atlantic by otolith shape
555 analysis. Can J Fish Aquat Sci. 73, 1–9.
556 Menezes, G.M., Sigler, M.F., Silva, H.M., Pinho, M.R., 2006. Structure and zonation of demersal fish assemblages
557 off the Azores Archipelago (mid-Atlantic). Mar. Ecol. Prog. Ser. 324, 241–260.
558 Mérigot, B., Letourneur, Y., Lecomte-Finiger, R., 2007. Characterization of local populations of the common sole
559 *Solea solea* (Pisces, Soleidae) in the NW Mediterranean through otolith morphometrics and shape analysis.
560 Mar. Biol. 151, 997–1008.
561 Meyer, A., 1987. Phenotypic plasticity and heterochrony in *Cichlasoma managuense* (Pisces, Cichlidae) and their
562 implications for speciation in cichlid fishes. Evolution. 41, 1357–1369.
563 Moreira, C., Froufe, E., Sial, A.N., Caeiro, A., Vaz-Pires, P., Correia, A.T., 2018. Population structure of the blue
564 jack mackerel (*Trachurus picturatus*) in the NE Atlantic inferred from otolith microchemistry. Fish. Res. 197,
565 113–122.
566 Moreira, C., Froufe, E., Vaz-Pires, P., Correia, A.T., 2019a. Otolith shape analysis as a tool to infer the population
567 structure of the blue jack mackerel, *Trachurus picturatus,* in the NE Atlantic. Fish. Res. 209, 40–48.
568 Moreira, C., Correia, A.T., Vaz-Pires, P., Froufe, E., 2019b. Genetic diversity and population structure of the blue
569 jack mackerel *Trachurus picturatus* across its western distribution. J. Fish Biol. in press.
570 Moyano, M., Hernández-León, S., 2009. Temporal and along-shelf distribution of the larval fish assemblage at
571 Gran Canaria, Canary Islands, in: Clemmesen, C., Malzahn, A.M., Peck, M.A., Schnack, D. (Eds.), Advances
572 in early life history study of fish. Scientia Marina, Barcelona, pp. 85–96.
573 Moyano, M., Hernández-León, S., 2011. Intra- and interannual variability in the larval fish assemblage off Gran
574 Canaria (Canary Islands) over 2005–2007. Mar. Biol. 158, 257–273.
575 Moyano, M., Rodríguez, J.M., Hernández-León, S., 2009. Larval fish abundance and distribution during the late
576 winter bloom off Gran Canaria Island, Canary Islands. Fish. Oceanogr. 18, 51–61.
577 Moyano, M., J.M. Rodríguez, V. Benítez-Barrios y S. Hernández-León, 2014. Larval fish distribution and
578 retention in the canary current system during the weak upwelling season. Fish. Oceanogr. 23 (3), 191–209.
579 Naish, K.A., Hard, J.J., 2008. Bridging the gap between the genotype and the phenotype: linking genetic variation,
580 selection and adaptation in fishes. Fish Fish. 9, 396–422.
581 Nielsen, L.A., 1992. Methods of marking fish and shellfish. American Fisheries Society, Special Publication 23,
582 Bethesda, Maryland.
583 Ogle, D.H., 2016. Introductory Fisheries Analyses with R. Chapman & Hall/CRC, Boca Raton.

584 Parisi-Baradad, V., Lombarte, A., Garcia-Ladona, E., Cabestany, J., Piera, J., Chic, Ò., 2005. Otolith shape contour
585 analysis using affine transformation invariant wavelet transforms and curvature scale space representation.
586 Mar. Freshw. Res. 56, 795–804.
587 Pérez-Quiñonez, C.I., Quiñonez-Velázquez, C., García-Rodríguez, F.J., 2018. Detecting *Opisthonema libertate*
588 (Günther, 1867) phenotypic stocks in northwestern coast of Mexico using geometric morphometrics based on
589 body and otolith shape. Lat. Am. J. Aquat. Res. 46 (4), 779–790.
590 Pigliucci, M., 2005. Evolution of phenotypic plasticity: where are we going now? Trends Ecol. Evol. 20, 481-486.
591 R Core Team, 2016. R: a language and environment for statistical computing. Vienna, Austria: R Foundation for
592 Statistical Computing. http://www.r-project.org.
593 Radhakrishnan, K.V., Yuxuan, L., Jayalakshmy, K.V., Liu, M., Murphy, B.R., Xie, S.G., 2012. Application of
594 otolith shape analysis in identifying different ecotypes of *Coilia ectenes* in the Yangtze Basin. China. Fish.
595 Res. 125, 156–160.
596 Ramler, D., Mitteroecker, P., Shama, L., Wegner, K., Ahnelt, H., 2014. Nonlinear effects of temperature on body
597 form and developmental canalization in the threespine stickleback. J. Evol. Biol. 27, 497–507.
598 Reichenbacher, B., Feulner, G.R., Schulz-Mirbach, T., 2009. Geographic variation in otolith morphology among
599 freshwater populations of *Aphanius dispar* (Teleostei, Cyprinodontiformes) from the Southeastern Arabian
600 Peninsula. J. Morph. 270, 469–484.
601 Reichenbacher, B., Reichard, M., 2014. Otoliths of five extant species of the annual Killifish *Nothobranchius* from
602 the East African Savannah. PLoS ONE 9, e112459.
603 Réveillac, E., Lacoue-Labarthe, T., Oberhänsli, F., Teyssié, J.L., Jeffree, R., Gattuso, J.P., Martin, S., 2015. Ocean
604 acidification reshapes the otolith-body allometry of growth in juvenile sea bream. J. Exp. Mar. Biol. Ecol. 463,
605 87–94.
606 Reznick, D., Lindbeck, E., Bryga, H., 1989. Slower growth results in larger otoliths: an experimental test with
607 guppies (*Poecilia reticulata*). Can. J. Aquat. Sci. 46, 108–112.
608 Rodgveller, C.J., Hutchinson, C.E., Harris, J.P., Vulstek, S.C., Guthrie, C.M., III, 2017. Otolith shape variability
609 and associated body growth differences in giant grenadier, *Albatrossia pectoralis*. PLoSONE 12(6), e0180020.
610 Ruas, J.C., Vaz-dos-Santos, A.M., 2017. Age structure and growth of the rough scad, *Trachurus lathami*
611 (Teleostei: Carangidae), in the Southeastern Brazilian Bight. Zoologia. 34, e20475.
612 Sadighzadeh, Z., Tuset, V.M., Valinassab, T., Dadpour, M.R., Otero-Ferrer, J.L., Lombarte, A., 2012. Comparison
613 of different otolith shape descriptors and morphometrics in the identification of closely related species of
614 *Lutjanus* spp. from the Persian Gulf. Mar. Biol. Res. 8, 802–814.
615 Sadighzadeh, Z., Otero-Ferrer, J.L., Lombarte, A., Fatemi, M.R., Tuset, V.M., 2014. An approach to unraveling
616 the coexistence of snappers (Lutjanidae) using otolith morphology. Sci. Mar. 78, 353–362.
617 Sassa, C., Konishi, Y., Tsukamoto, Y., 2016. Interannual var- iations in distribution and abundance of Japanese
618 jack mackerel *Trachurus japonicus* larvae in the East China Sea. ICES J. Mar. Sci. 73, 1170–1185.
619 Secor, D.H., 1999. Specifying divergent migrations in the concept of stock: the contingent hypothesis. Fish. Res.
620 43, 13–34.
621 Secor, D.H., 2002. Historical roots of the migration triangle. ICES J. Mar. Sci. 215, 329–335.
622 Secor, D.H., 2005. Fish migration and the unit stock: three formative debates, in: Cadrin, S.X., Friedland, K.D.,
623 Waldman, J.R. (Eds.), Stock identification methods. Applications in Fishery Science. Elsevier, Amsterdam,
624 pp. 17-44.
625 Secor, D.H., Dean, J.M., 1989. Somatic growth effects on the otolith-fish size relationship in young pond-reared
626 striped bass, *Morone saxatilis*. Can. J. Fish. Aquat. Sci. 46, 113–121.
627 Schluter, D., 1995. Adaptive radiation in sticklebacks - trade-offs in feeding performance and growth. Ecology
628 76, 82–90.
629 Shaboneyev, I.Y., Ryazantseva, Y.I., 1977. Population structure of the oceanic horse mackerel (*Trachurus*
630 *picturatus*). J. Ichthyol. 17, 954–958.
631 Skulason, S., Noakes, D.L., Snorranson, S.S., 1989. Ontogeny of trophic morphology in four sympatric morphs of
632 Arctic charr *Salvelinus alpinus* in Thingvallavatn, Iceland. Biol. J. Linn. Soc. 38, 281–301.
633 Smith-Vaniz, W., Berry, F.H., 1981. Carangidae, in: Fischer, W., Bianchi, G., Scott, W.B. (Eds.), FAO species
634 identification sheets for fishery purpose - Fishing areas 34, 47 (in part) (Eastern Central Atlantic) (Vols. 1,
635 Bony fishes). Funds-in-Trust, Canada.
636 Stransky, C., MacLellan, S.E., 2005. Species separation and zoogeography of redfish and rockfish (genus
637 *Sebastes*) by otolith shape analysis. Can. J. Fish Aquat. Sci. 62, 2265–2276.
638 Stransky, C., Baumann, H., Fevolden, S.E., Harbitz, A., Høie, H., Nedreaas, K.H., Salberg, A.B., Skarstein, T.,
639 2008. Separation of Norwegian coastal cod and Northeast Arctic cod by outer otolith shape analysis. Fish. Res.
640 90, 26–35.
641 Sturrock, A.M., Trueman, C.N., Darnaude, A.M., Hunter, E., 2012. Can otolith elemental chemistry
642 retrospectively track migrations in fully marine fishes? J. Fish Biol. 81, 766–795.
643 Swain, D.P., Foote, C.J., 1999. Stocks and chameleons: the use of phenotypic variation in stock identification.
644 Fish. Res. 43, 113–128.

Tanner, S.E., Reis-Santos, P., Cabral, H.N., 2015. Otolith chemistry in stock delineation: a brief overview, current challenges and future prospects. Fish. Res. 173, 206–213.
Thorrold, S.R., Campana, S.E., Jones, C.M., Swart, P.K., 1997. Factors determining $\delta^{13}C$ and $\delta^{18}O$ fractionation in aragonite otoliths of marine fish. Geochim. Cosmochim. Acta. 61, 2909–2919.
Thorrold, S.R., Zacherl, D.C., Levin, L.A., 2007. Population connectivity and larval dispersal using geochemical signatures in calcified structures. Oceanography. 20, 80–89.
Turan, C., 2006. The use of otolith shape and chemistry to determine stock structure of Mediterranean horse mackerel *Trachurus mediterraneus* (Steindachner). J. Fish Biol. 69 (Suppl. C), 165–180.
Tuset, V.M., Lombarte, A., González, J.A., Pertusa, J.F., Lorente, M.J., 2003. Comparative morphology of the sagittae otolith in *Serranus* spp. J. Fish Biol. 63, 1491–1504.
Tuset, V.M., González, J.A., Lozano, I.J., García-Díaz, M.M., 2004. Age and growth of the blacktail comber, *Serranus atricauda* (Serranidae), off the Canary Islands (central-eastern Atlantic). Bull. Mar. Sci. 74, 53–68.
Tuset, V.M., Imondi, R., Aguado, G., Otero-Ferrer, J.L., Santschi, L., Lombarte, A., Love, M., 2015. Otolith patterns of rockfishes from the northeastern pacific. J. Morphol. 276, 458–469.
Tuset, V.M., Otero-Ferrer, J.L., Stransky, C., Imondi, R., Orlov, A., Zhenjiang, Y., Venerus, L., Santschi, L., Afanasiev, P., Zhuang, L.O., Farré, M., Love, M., Lombarte, A., 2016. Otolith shape lends support to the sensory drive hypothesis in rockfishes. J. Evol. Biol. 29 (10), 2083–2097.
Vasconcelos, J., Alves, A., Gouveia, E., Faria, G., 2006. Age and growth of the blue jack mackerel, *Trachurus picturatus* Bowdich, 1825 (Pisces: Teleostei) off Madeira archipelago. Arquipel. Life Mar. Sci. 23A, 47–57.
Vasconcelos, J., Hermida, M., Saraiva, A., González, J.A., Gordo, L.S., 2017. The use of parasites as biological tags for stock identification of blue jack mackerel, *Trachurus picturatus*, in the north-eastern Atlantic. Fish. Res. 193, 1–6.
Vasconcelos, J., Vieira, A.R., Sequeira, V., González, J.A., Kaufmann, M., Serrano Gordo, L., 2018. Identifying populations of the blue jack mackerel (*Trachurus picturatus*) in the Northeast Atlantic by using geometric morphometrics and otolith shape analysis. Fish. Bull. 116, 81-92.
Vignon, M., 2012. Ontogenetic trajectories of otolith shape during shift in habitat use: interaction between otolith growth and environment. J. Exp. Mar. Biol. Ecol. 420−421, 26−32.
Vignon, M. 2015. Disentangling and quantifying sources of otolith shape variation across multiple scales using a new hierarchical partitioning approach. Mar. Ecol. Progr. Ser. 534, 163–177.
Vignon, M., Morat, F. 2010. Environmental and genetic determinant of otolith shape revealed by a non-indigenous tropical fish. Mar. Ecol. Progr. Ser. 411, 231–241.
Von Bertalanffy L., 1938. A quantitative theory of organic growth. Hum Biol. 10 (2), 181–243.
Ward, T.D., Algera, D.A., Gallagher, A.J., Hawkins, E., Horodysky, A., Jørgensen, C., Killen, S.S., McKenzie, D.J., Metcalfe, J.D., Peck, M.A., Vu, M., Cooke, S.J., 2016. Understanding the individual to implement the ecosystem approach to fisheries management. Conserv. Physiol. 4, 1–10.
Worthington, D.G., Doherty, P.J., Fowler, A.J., 1995. Variation in the relationship between otolith weight and age: implications for the estimation of age of two tropical damselfish (*Pomacentrus moluccensis* and *P. wardi*). Can. J. Fish. Aquat. Sci. 52, 233–242.
Yao, H., Duan, Q., Li, D., Wang, J., 2013. An improved K-means clustering algorithm for fish image segmentation. Math. Comput. Mod. 58(3), 790–798.
Zar, J.H., 1996. Biostatistical Analysis. Prentice-Hall International, New Jersey.
Zenkin, V.S., Ryazantseva, E.I., 1987. Biochemical genetic aspects of studying the population structure of the east Atlantic horse mackerel *Trachurus picturatus* (Bowdich). ICES CM/H:23, 1–18.

Legends

Fig. 1. Geographical location of *Trachurus picturatus* sampled off the north-eastern Atlantic Ocean. Arrows indicates theoretical hypotheses on the stock mixing in the Canary Islands.

Fig. 2. Decomposition of otolith contour using wavelet functions in *Trachurus picturatus* from the Canary Islands (NE Atlantic Ocean). X-axis is the 512 equidistant points of contour; Y-axis represents the mean normalized distance. The wavelets 4 were used for the identification of stocks following Sadighzadeh *et al*. (2014).

Fig. 3. (a) Scatterplot of the first and second axes of the PCA and marginal density distribution plots of the three otolith phenotypes found in *Trachurus picturatus* from the Canary Islands (NE Atlantic Ocean); (b) Average decomposition of otolith contour of the three phenotypes showing the zones with higher intraspecific variability. Colour circles indicate the centroid of each morphotype.

Fig. 4. Temporal and ontogenetic variability of the three otolith phenotypes found in *Trachurus picturatus* from the Canary Islands (NE Atlantic Ocean). Ad., adult; Juv., juvenile. Breeding, January-April; Feeding, May-July; Recruitment, August-December (Jurado-Ruzafa and Santamaría, 2011, 2013). The percentage and number of specimens (in parenthesis) by group are given.

Fig. 5. Frequency distributions by fish age and size of the three otolith phenotypes found in *Trachurus picturatus* from the Canary Islands (NE Atlantic Ocean).

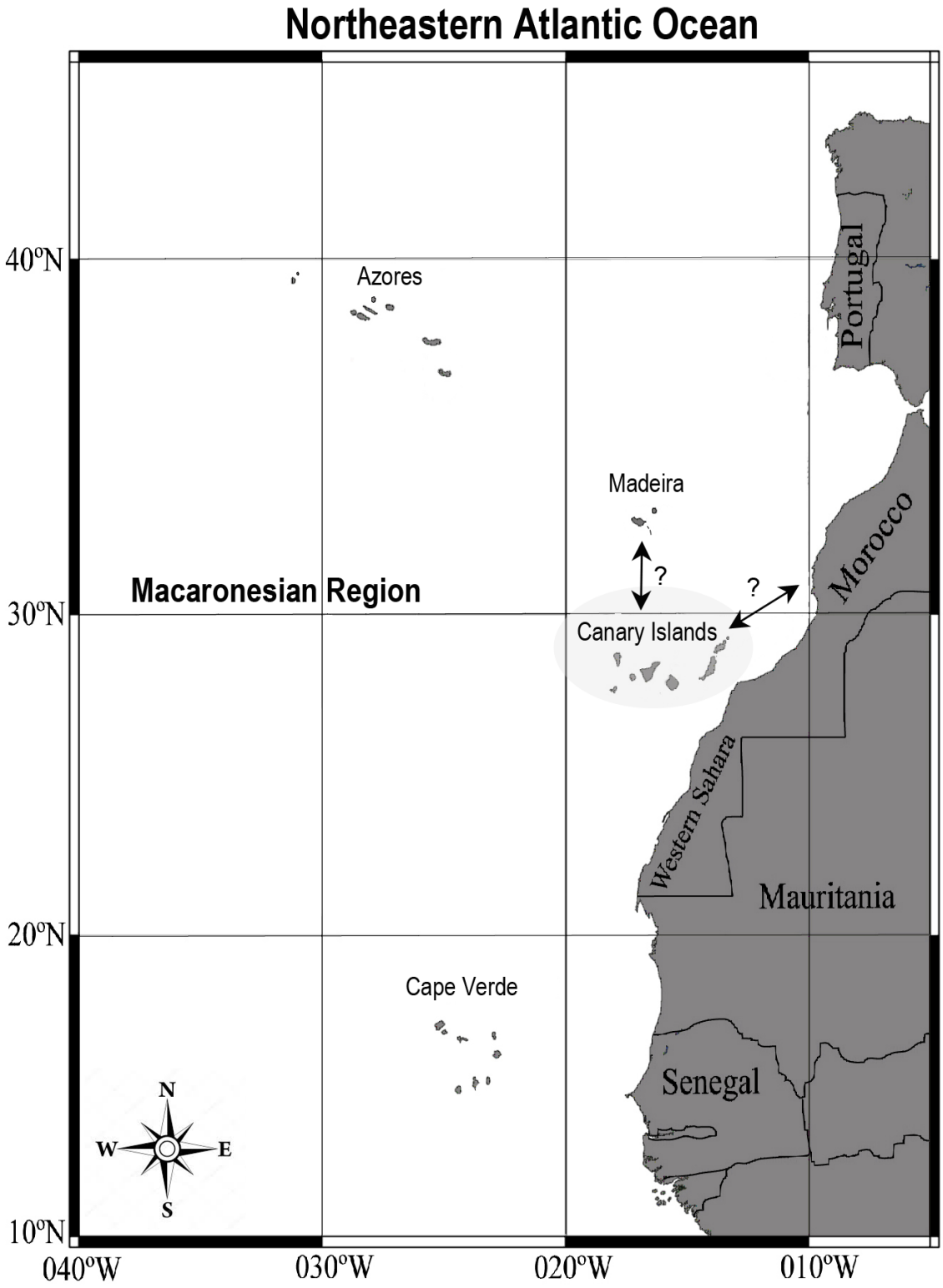

720

721

722

723

724

725

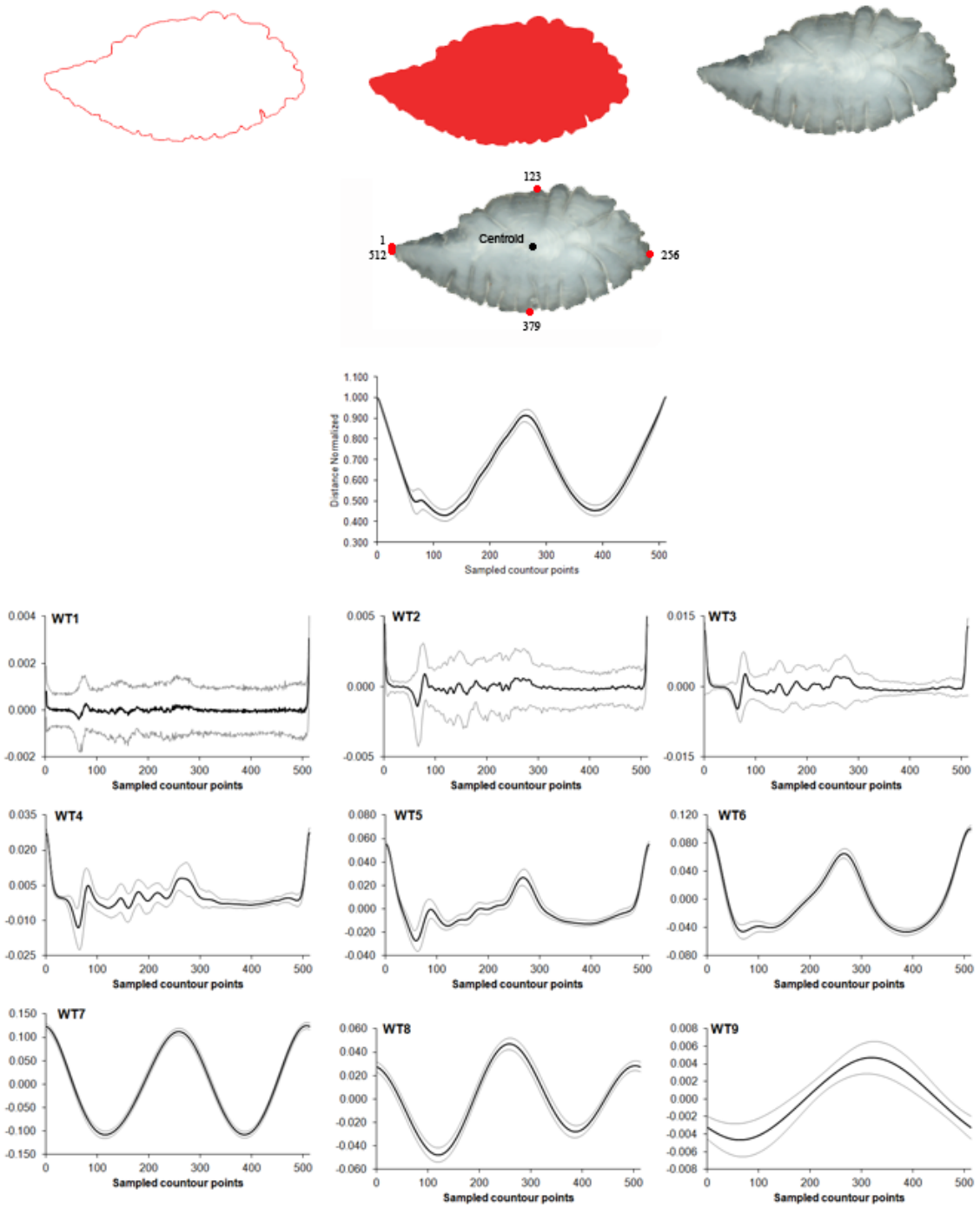

726

727

728

729

730

731

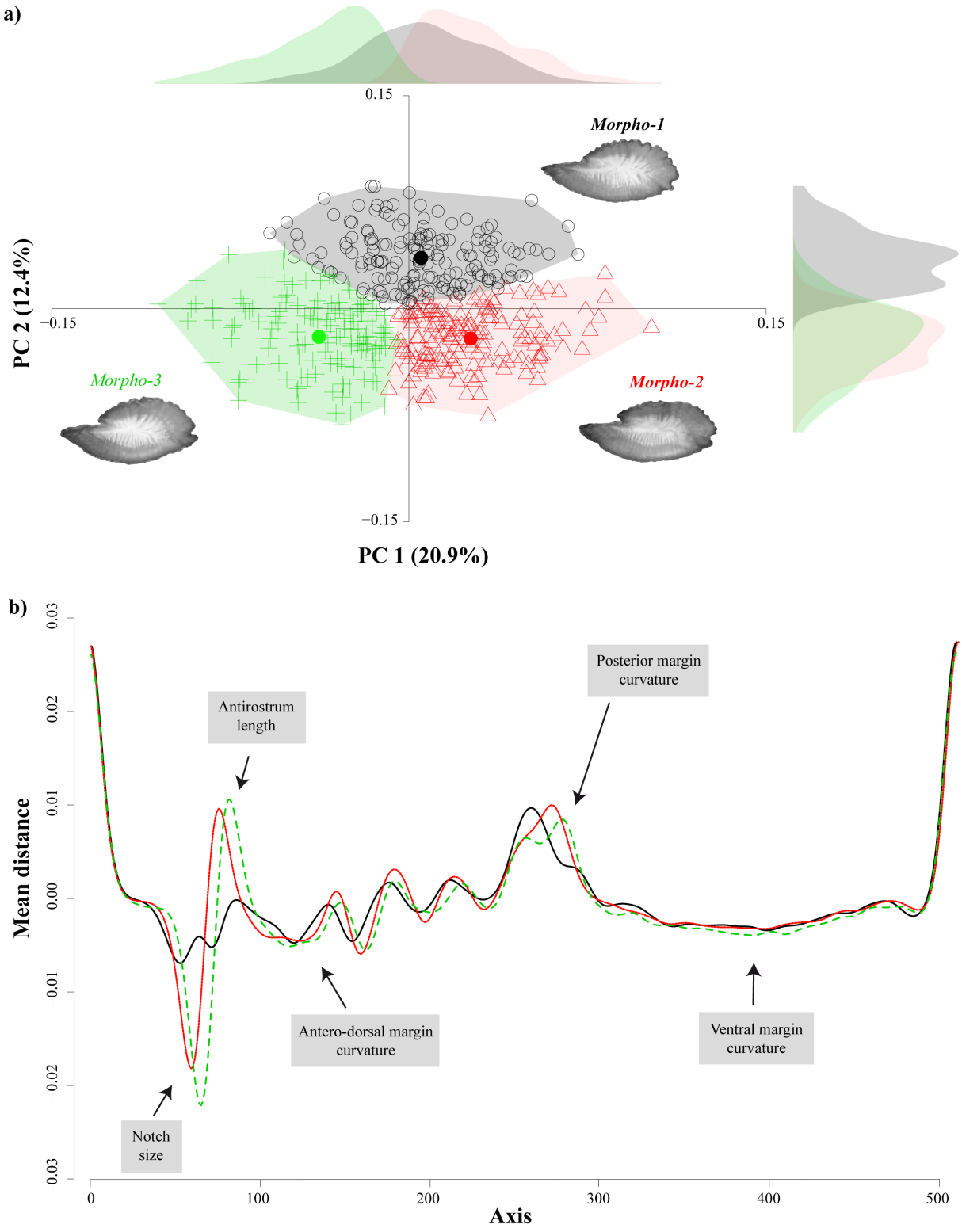
a)
0.15
Morpho-1
PC 2 (12.4%)
−0.15
0.15
Morpho-3
Morpho-2
−0.15
PC 1 (20.9%)
b)
Mean distance
0.03
0.02
0.01
0.00
−0.01
−0.02
−0.03
Antirostrum length
Posterior margin curvature
Antero-dorsal margin curvature
Ventral margin curvature
Notch size
0
100
200
300
400
500
Axis

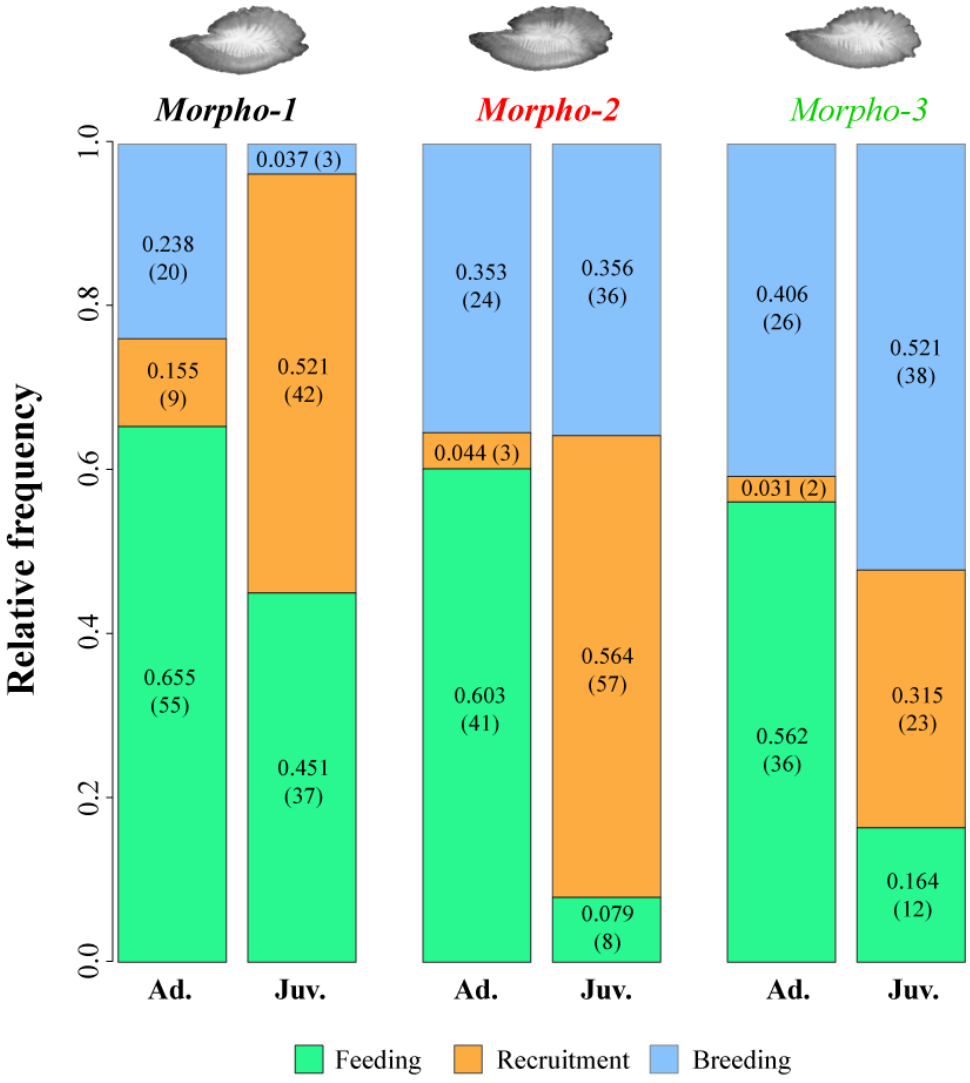
Morpho-1
Morpho-2
Morpho-3
Relative frequency
0.0
0.2
0.4
0.6
0.8
1.0
0.238 (20)
0.155 (9)
0.655 (55)
0.037 (3)
0.521 (42)
0.451 (37)
0.353 (24)
0.044 (3)
0.603 (41)
0.356 (36)
0.564 (57)
0.079 (8)
0.406 (26)
0.031 (2)
0.562 (36)
0.521 (38)
0.315 (23)
0.164 (12)
Ad.
Juv.
Ad.
Juv.
Ad.
Juv.
Feeding
Recruitment
Breeding

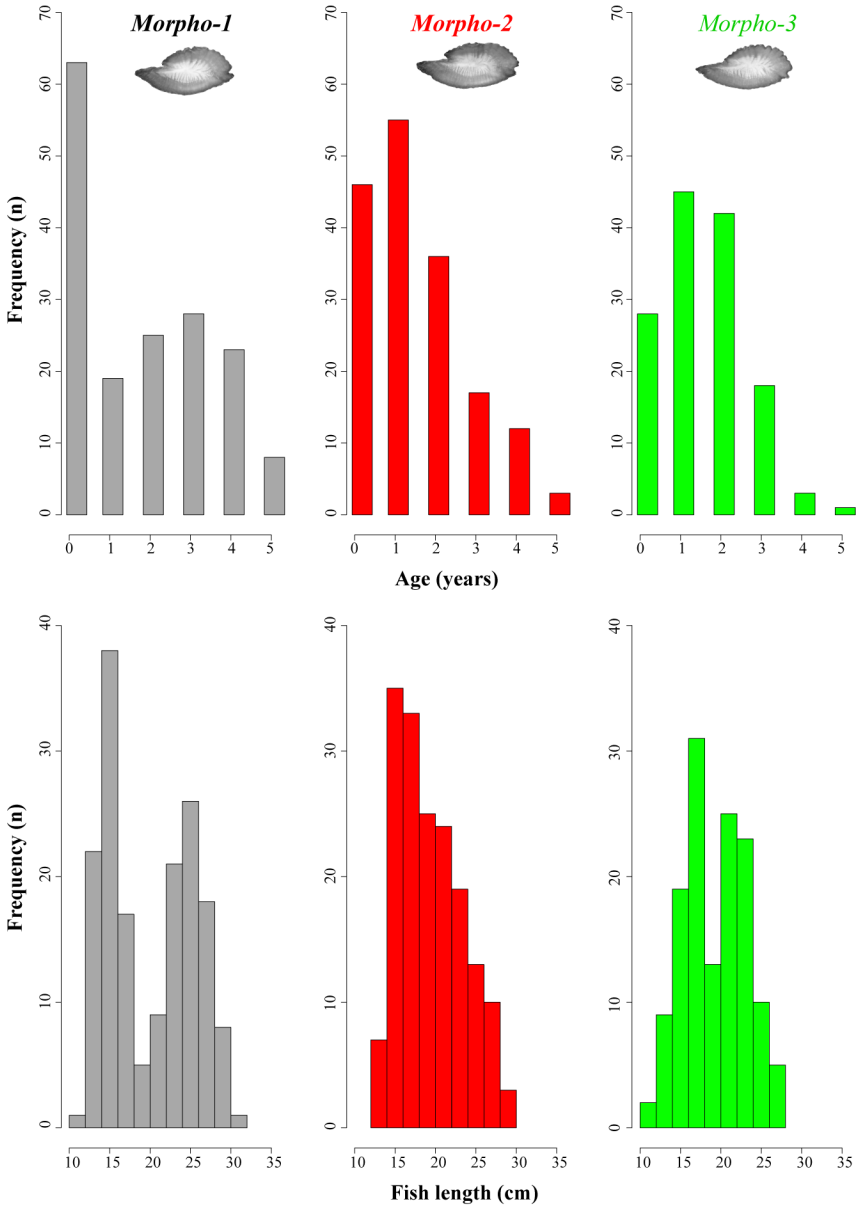
Morpho-1
Morpho-2
Morpho-3
Frequency (n)
Age (years)
Frequency (n)
Fish length (cm)

Table 1

Mean comparison of the fish and otolith length and age between morphotypes of *Trachurus picturatu*s from the Canary Islands (NE Atlantic Ocean). n, number of individuals; ns, non-significant; *OL*, otolith length; *TL*, total length.

	Morphotype 1 (n= 166)			*Morphotype 2* (n= 169)			*Morphotype 3* (n= 137)			Kruskall-Wallis test
Variable	min.	max.	mean ± sd	min.	max.	mean ± sd	min.	max.	mean ± sd	
TL (cm)	11.3	32	20.01 ± 5.40	12.4	28.9	19.46 ± 4.00	10.4	27.2	19.29 ± 3.76	0.328 (ns)
OL (mm)	3.20	8.67	5.80 ± 1.44	3.93	8.53	5.79 ± 1.05	2.94	7.53	5.70 ± 0.97	0.158 (ns)
Age (years)	0	5	1.72 ± 1.65	0	5	1.43 ± 1.28	0	5	1.46 ± 1.07	0.375 (ns)

Table 2

Estimation of the von Bertalanffy growth parameters using the otolith reading method for the morphotypes of *Trachurus picturatus* from the Canary Islands (NE Atlant Ocean). C.I., confidence intervals; k, growth rate (year^{-1}); L_{inf}, asymptotic length (cm); n, number of individuals; ns, non-significant; t_0, time (year).

		Non-fixing			Fixing L_{inf}			Fixing k		
Parameters		*Morphotype 1* (n=166)	*Morphotype 2* (n=169)	*Morphotype 3* (n=137)	*Morphotype 1* (n=166)	*Morphotype 2* (n=169)	*Morphotype 3* (n=137)	*Morphotype 1* (n=166)	*Morphotype 2* (n=169)	*Morphotype 3* (n=137)
L_{inf}	Estimate	32.46	40.95	29.64		33.25		34.03	32.54	32.55
	Standar error	1.84	7.19	2.38		1.56		1.63	1.57	1.74
	Lower 2.5% C.I.	28.85	27.05	24.96		30.16		30.83	29.45	29.17
	Upper 97.5% C.I.	35.94	54.04	34.35		36.31		37.23	35.63	36.00
k	Estimate	0.28	0.14	0.32	0.26	0.23	0.24		0.25	
	Standar error	0.05	0.05	0.08	0.04	0.03	0.03		0.03	
	Lower 2.5% C.I.	0.19	0.05	0.17	0.19	0.17	0.18		0.18	
	Upper 97.5% C.I.	0.38	0.25	0.47	0.34	0.29	0.29		0.30	
t_o	Estimate	-2.04	-3.21	-2.00	-2.11	-2.58	-2.36	-2.20	-2.47	-2.32
	Standar error	0.21	0.49	0.30	0.18	0.22	0.20	0.17	0.20	0.19
	Lower 2.5% C.I.	-2.44	-4.08	-2.59	-2.46	-3.00	-2.76	-2.53	-2.85	-2.69
	Upper 97.5% C.I.	-1.62	-2.24	-1.42	-1.76	-2.16	-1.96	-1.87	-2.08	-1.96

779

780

781
782 **Supplementary material**

783
784
785
786
787
788
789
790
791
792
793
794
795
796

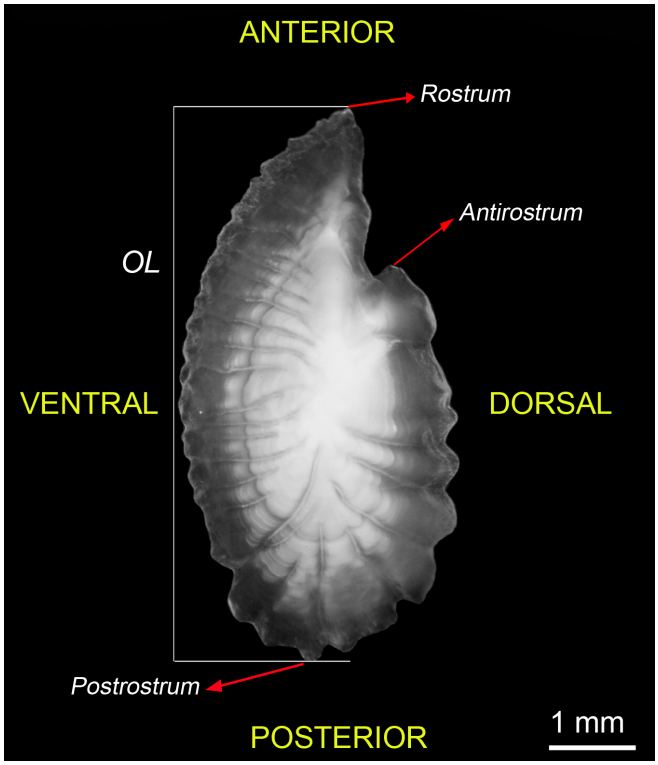

797
798 **Fig. S1.** Lateral surface of *sagittae* otoliths of *Trachurus picturatus* from the Canary Islands
799 (NE Atlantic Ocean) illustrating features considered.
800

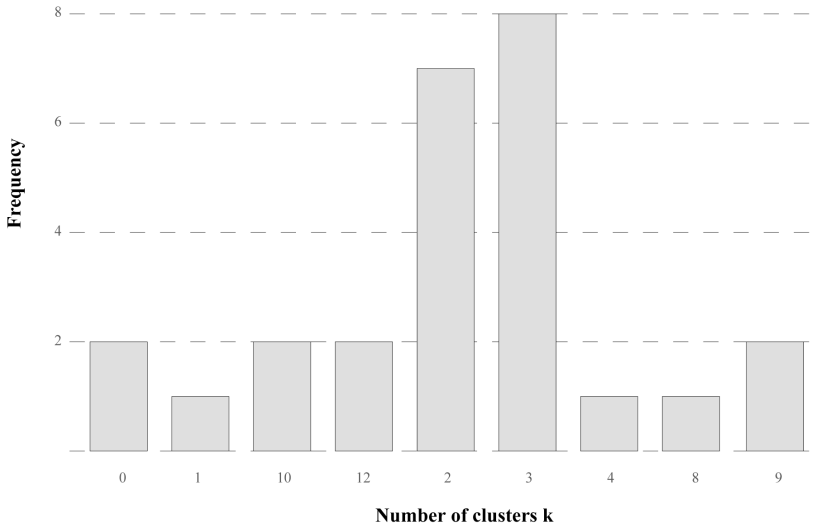

801
802 **Fig. S2.** Determination of clusters obtained by *K*-means analysis.
803
804

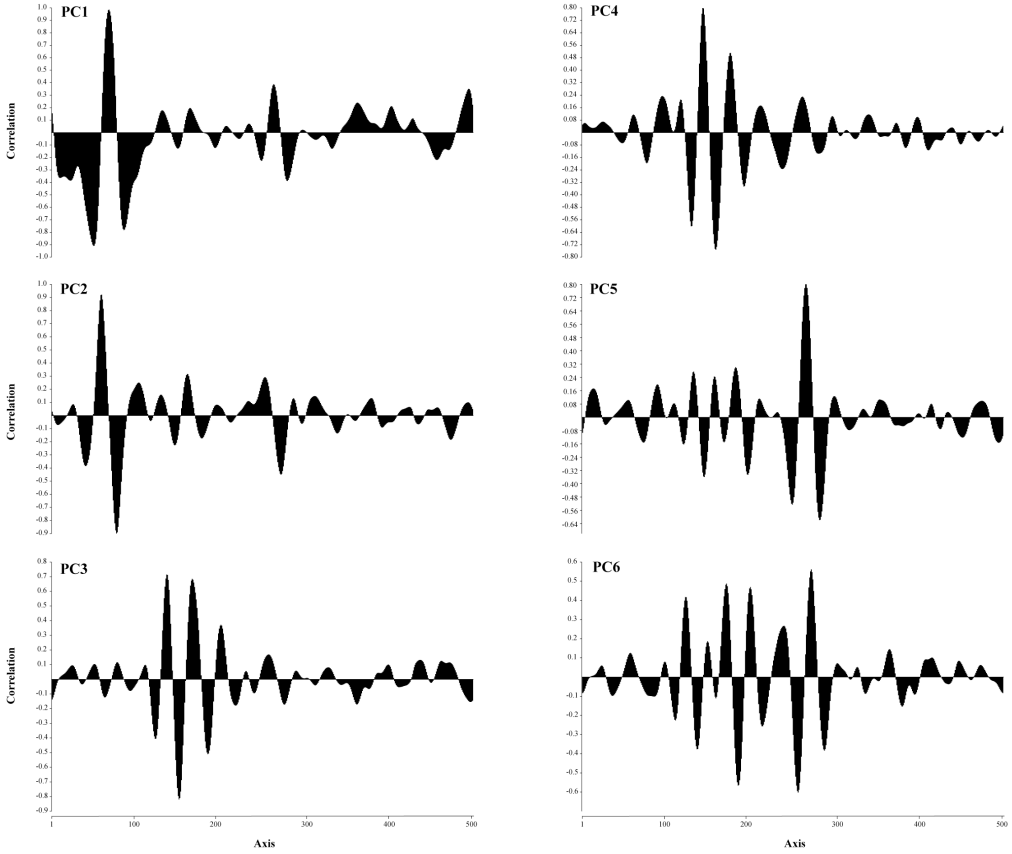

Fig. S3. Correlation values between the points of otolith contour (n= 512) and the first six PC components.

Table S1

Variance explained by Principal components (PC) derived from otolith shape analysis of *Trachurus picturatus* from the Canary Islands (NE Atlantic Ocean).

PC	Eigenvalue	Variance (%)
1	0.00195	20.38
2	0.00121	12.64
3	0.00065	6.81
4	0.00062	6.44
5	0.00059	6.13
6	0.00052	5.46
7	0.00046	4.81
8	0.00037	3.85
9	0.00026	2.71
10	0.00023	2.35
11	0.00022	2.28
12	0.00020	2.10
13	0.00018	1.87
14	0.00017	1.77
15	0.00016	1.65
16	0.00014	1.50
17	0.00013	1.36
18	0.00012	1.25
19	0.00011	1.18
20	0.00010	1.04
21	0.00009	0.97
22	0.00009	0.95
23	0.00009	0.92
24	0.00007	0.75
25	0.00006	0.68
26	0.00006	0.65
27	0.00006	0.58
Total		93.09